NSEMX_Conf2021_031

Synthesis of Ni-Al2O3 Nanocatalyst for Low Temperature Production of Carbon Nanotubes (CNTs)

Yerima, M. L[1]., Abdulkareem A. S[2]., Abubakre, O. K[3], Ndaliman, M. B[4]. Khan, R. H.[5], and Muriana, R.A.[6]

Material and Metallurgical Department, Federal University of Technology, Minna, Nigeria[1, 6]
Chemical Engineering Department, Federal University of Technology Minna, Nigeria[2]
Mechanical Engineering Department, Baze University, Abuja, Nigeria[5]
Mechanical Engineering Department, Federal University of Technology, Minna, Nigeria[3, 4,]

ABSTRACT

This study focused on the synthesis of nickel - aluminium oxide support (Ni-Al_2O_3) nanocatalyst by wet impregnation method. The catalyst yield of 86.00 % was obtained at temperature of 400 ^{O}C for 3 hours after calcination. The catalyst was characterized to determine the thermal property, Morphology, crystalinity, pore volume/particle size and surface area using TGA, SEM/EDX, XRD, DLS and BET respectively. Results obtained revealed that the catalyst produced has an average particle size of 82.24 nm. It was highly crystalline with BET surface area of 428.352 m^2/g, pore size of 0.2817 Â and pore volume of 0.1779 cc/g. Analysis of the results also shows that the catalyst developed is thermally stable with about 0.5% wt loss at 800 ^{O}C, which makes the catalyst suitable for CNTs production. The catalyst developed was used to produce carbon nanotubes at operating temperature of 600 ^{O}C with argon flow rate of 30ml/min, acetylene flow rate of 300 ml/min and production time of 55 minutes. The results obtained revealed that the yield of 135 % was obtained. The CNTs produced was characterized and the results shows that the produced CNTs is thermally stable with BET surface area of 833.64 m^2/g, pore volume of 0.3286 cc/g and pore size of 0.3148 Â. This study demonstrated that employing Ni-Al_2O_3 nanocatalyst provides suitable route for efficient low temperature production of CNTs.

KEYWORDS: Nickel, Aluminium oxide, characterization, CVD, CNTs

1 INTRODUCTION

Since its discovery, Carbon nanotubes (CNTs) has continued to attract research interest worldwide. After its discovery by Sumio Iijima in 1991, this novel nanostructure material has gained recognition due to its wonderful physical properties that makes it suitable for many unique applications (Toussi *et al.,* 2011) in many fields of engineering. CNTs are nanoscale carbon structure that could be described as graphene sheets rolled up into the shape like of a cylinder (Bondi *et al.,* 2005) with one end covered with hemisphere of the fullerene structure (Arranz-Andréas and Blau, 2010). Regardless of the type of CNTs which are single walled carbon nanotube and multiwalled carbon nanotube (Werner and Andreas 2004); they generally have common methods of synthesis. Owing to its many intriguing properties, the production of CNT has turn out to be a significant subject of worldwide research. Carbon nanotubes (CNTs) are especially promising over various existing materials inferable from their interesting unique/ anisotropic extraordinary chemical, electrical, thermal and mechanical properties (Afolabi *et al.*, 2014) that have caught creative energy of scientists globally since their revelation by Sumio Iijima in (1991). Owing to these remarkable electrical properties and very extraordinary thermal conductivity, CNTs was utilized for energy storage, functional fillers in composites field-emission displays, some biomedical devices and electronics (Muhammad *et al.,* 2011; Ajayan, 2001; Baughman *et al.,* 2002). Additionally, CNTs have great flexible moduli (>1TPa), huge expandable straining length equal to 5 percent, with huge breaking strain up to 20 percent (Esfarjani, 2013). It's their outstanding mechanical properties may conceivably pilot an excess of many uses. For instance, with their noteworthy stiffness and strength and adding to the advantage of lightness, standpoint prospect applications of CNTs are in progressive plane design (aerospace engineering), biomedical engineering (virtual bio-devices) and other disciplines.

Different support materials such as Al_2O_3, zeolite, MgO, SiO_2, and $CaCO_3$ have been applied as a carrier in supported-catalysts for CNT (Kathyayini *et al., 2008;* Willems*et al.,* 2000; *Mao-Lin et al.,* 2012 and Couteau*et al.,* 2003). Several researchers have reported high purity multi-walled carbon nanotubes obtained from Co-Mo supported MgO catalyst via CVD Peleche*t al.,* 2009; Quian*et al.,*2003; Yeoh*et al.,*2009). Awadallah*et al. (*2012) demonstrated the synthesis of CNTs prepared via CVD methods from Ni-Mo and Co-Mo supported on Al2O3 catalyst. Studies have shown that alumina supported catalysts for CNTs synthesis appeared more promising due creation of a high surface areas and mesoporous materials which promote catalysis (Kathyayini*et al., 2008*). In addition, Al_2O_3 has good thermal stability and can be easily removed after the synthesis via acid purification. In this present study, bi-metallic Fe-Ni catalyst supported on aluminium oxide were developed and utilised to prepare CNT through CVD method. The choice Ni as an active part of the catalyst is due to it availability and cheapness (Uddin *et al., 2008*).

2.0 METHODOLOGY

2.1 Materials

The chemicals used in this work are of high grade with high purity, ranging from 98.5- 99.99 %. These chemicals include nickel nitrate hexahydrate ($Ni(NO_3)_2.6H_2O$), alumina (Al_2O_3), distilled water and concentrated hydrochloric acid (H_2SO_4) were supplied by Aldrich. The carbon source (acetylene) and carrier gas (argon) are also of analytical grade with 99.99% purity supplier by BOC Nigeria.

2.1.1 Catalyst Synthesis

The catalyst was prepared by wet impregnation methods. A 0.22 mol/dm^3 aqueous solution of Ni $(NO_3)_2.6H_2O$ with IUPAC Name Nickel (II) nitrate hexahydrate (salt solution) was made by impregnating support material (Al_2O_3 powder) in the salt solution. For single metallic Ni based catalysts, Ni $(NO_3)_2.6H_2O$/aqueous solution was used. Molar ratio of Ni: Al_2O_3) 1:2 was used in preparing the catalyst systems. The following describes the detailed procedure for preparing a Ni/Al_2O_3 catalyst. Support material (5-6 g) was suspended in 50 ml of deionized water with stirring, followed by the addition of 3.198 g of a green Ni $(NO_3)_2.6H_2O$. The mixture was allowed to stir for 20 min. and the resulting slurry was dried in an oven at 120 ^{0}C – 125 ^{0}C for 5 to 7 hrs. After drying, the material was grinded with an agate mortal to obtain fine light green powder. It was then calcined in muffle furnace at 400 ^{0}C for 2hr, cooled to room temperature, and re-grinded prior to CVD growth. The calcined material (grey) was sieved using a sieve of 150 micrometer and the desired catalyst was collected as fine particles. The percentage yield of the catalyst before oven drying (Yield Dried), and after calcination (Yield Calcined) is calculated using equation 1 and 2;

$$Yield\ (\%) = \left(\frac{Mass\ of\ catalyst\ \ after\ oven - drying}{Mass\ after\ oven\ drying}\right) \times\ 100 \qquad 1$$

$$Yield\ (\%) = \left(\frac{Mass\ of\ catalyst\ \ after\ calcination - drying}{Mass\ after\ oven\ drying}\right) \times 100 \qquad 2$$

2.1.2 Synthesis of CNTs

The horizontal CVD reactor equipment shown in Plate 1was used for the CNTs synthesis. It has a length of 1010 mm with internal and external diameter of 52 mm and 60 mm respectively. 1.0 g of the supported bimetallic catalyst (Ni/Al_2O_3) was weighed and spread evenly on a quartz boat placed at the central part of the horizontal tube.

Plate 1: The horizontal CVD set up for the synthesis of carbon nanotubes

The heating rate, temperature, gas flow rates were maintained at the desired rate. The entrapped gases in the quartz tube were expelled using argon as the carrier gas at a flow rate of 30 ml/min. At a temperature of 600 0C, the flow of acetylene was released into the quartz tube of catalytic reactor at 100 ml/min for 55 min with immediate increment in the flow rate of the carrier gas (argon) to 300 ml/min. As the residence time (45 minutes) of the reaction was attained, the flow of acetylene was stopped and the argon gas was left flowing at 30 ml/min until the reactor cooled to room temperature. The sample was removed, weighed and analysed. The yield of the deposited carbon was therefore determined using Equation (3) (Yeoh*et al.,* 2009; Taleshi, 2012).

$$CNTs\ Yield\ (\%) = \left(\frac{MTotal - MCatalyst}{MCatalyst}\right) \times 100 \quad (1)$$

2.2 Characterization

2.2.1 Thermo Gravimetric Analysis (TGA) and Differential Thermal Analysis (DTA)

The thermal stability, compositional and percentage purity of materials were determined using TGA 4000 (PerkinElmer). Samples were analyzed in nitrogen environment at a volumetric flow rate of 20 ml/min, pressure of 2.5 bars and heating rate of 10 ^{O}C/min. The thermal balance was zeroed, the sample was recorded and placed into the equipment utilizing pyris manager software. When constant weight was observed utilizing the formed heating profile, the analysis was then commenced. The test effects were then studied using pyris manager for proximate and compositional analysis.

2.2.2 X-Ray Diffraction Patterns (XRD)

Crystal phase identification of the catalyst and CNTs materials were studied utilising Bruker AXS D8 X-ray diffractometer system which was linked to Cu-Kα radiation of 40 kV and a current of 40 mA. The λ for Kα was 0.1541 nm, scanning rate was 1.5 º/min, The step width of 0.05° was used over 2θ range value of 20 – 80º.

2.2.3 High Resolution Scanning Electron Microscope (HRSEM)

The surface topology and the microstructure of the catalyst and CNTs was studied using Zeiss Auriga HRSEM. The HRSEM was equipped with EDS and it was used to obtain the elemental composition of the produced materials. A small quantity of the materials was sprinkled on a sample holder and sputter coated with Au-Pd using Quorum T15OT for 5 minutes before the analysis. The sputter coated samples was firmly attached to the carbon adhesive tape and studied using ZeissAuriga HRSEM equipped with In-lens standard detector at 30 kV.

2.2.4 BET Surface Area

The surface area of the synthesized catalyst was investigated by means of BET method in Nova e-series equipment. A sample weighing 300 mg was degassed at 150 o - 250 OC for 4 hrs in order to remove moisture. The degassed sample was then examined for physisorption of the adsorbate (nitrogen) by the adsorbent in liquid nitrogen environment.

2.2.5 Particle Size Analysis (DLS Technique)

In order to determine the particle size and the hydrodynamic diameter, Zeta Nanosizer was used at scattering angle of 173 ^{O} operating at 25 ^{O}C with equilibrating time of 120 secs. 1 mg of the samples were dispersed in 10 ml of ethanol then transferred into a polystyrene cuvette using a syringe with 0.22 µm filter coupled to it.

3 RESULTS AND DISCUSSION

The suitability of the nickel catalyst material for CNTs growth at CVD reaction temperature of about 600 ^{O}C was investigated by thermogravimetric analysis (TGA) and the thermal differential analysis (DTA) presented in Figure 1. The results as presented in Figure 1 shows that there were four regimes of weight losses in the TGA graph of the catalyst sample. The sample had continuous loss in weight from the initial temperature until 400 ºC. According to the differential thermogravimetric (DTG) curves this process is endothermic and can be attributed to elimination of water. In the regime of 400– 550 ºC the sample loss of weight was observed to be faster. This can be ascribed to the thermal decomposition of nickel nitrate hexahydrate as well as the formation of metal oxides (Lobiak *et al.,* 2014).

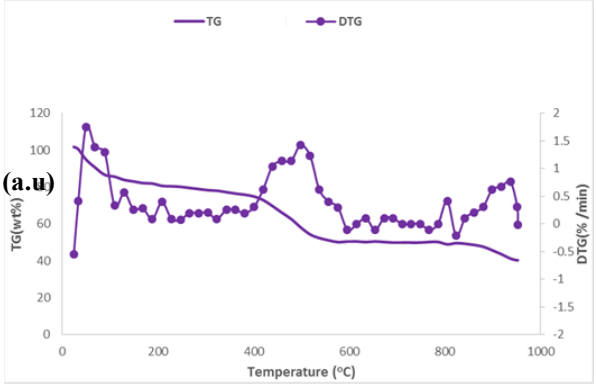

Figure 1: TGA and DTA curves of nickel catalyst obtained at 10 °C /min heating

Moreover, within these temperature ranges the DTG curves show the peaks corresponded to crystallization processes of metal oxides. In the following regime of 600 -850 °C the change of weight was not significant until 850 ^{0}C and above which exhibited another regime of steady weight loss.

The XRD analysis pattern of the calcined catalyst sample is presented in Figure 2, showed sharpened diffraction peaks that indicates that a growth has occurred in the crystallite size of NiO. This also suggests that the prepared catalyst is highly crystalline, an indication of orderly distribution of the metallic ions on the pore of the alumina support. Deep peaks matching the alumina support are detected for the catalysts. The aluminium oxide existed in the both α -Al_2O_3 and 𝛘 - Al_2O_3 form or as a combination of both. Metal oxide peaks were detected in catalyst

The major characteristics peak position appearing at 2θ= 19.1°, 27°, 31°, 36°, 37.10°, 43°.30°, 45°, 55°, 62.87°, 76.50° and 79.22° value respectively. The characteristics peak at 2θ value of 35. 23° suggest the presence of alpha alumina (α-Al_2O_3) (Kathyayini *et al.,* 2008) explaining that the pattern showed primarily the presence of peaks Al_2O_3 due to Nickel particles well dispersed on the surface of the Al_2O_3. This infers that the metal nanoparticles might have very small particle sizes in amorphous state and therefore unable to cause a Bragg reflection (Scherrer, 1918). This also conformed to the findings of (Tran *et al.,* 2007) who observed similar occurrence during the analysis of the XRD spectra obtained on the characterization of Ni/Al_2O_3.The sharpness and intensity of the peaks designates the well crystalline nature of the developed catalyst.

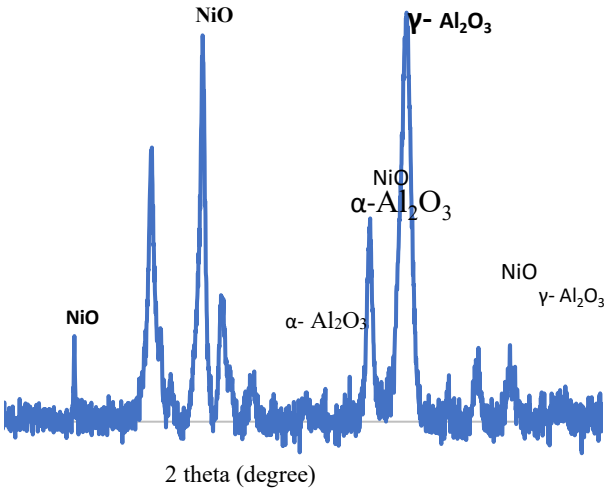

Figure 2: XRD spectra of Fe-Ni/Al_2O_3 catalyst

The particle size distribution of the synthesized supported catalyst based on the respective identified peaks in the XRD pattern is presented in Figure 2 In order to properly establish the phases that are present in the catalyst sample, comparison is made between peaks in its XRD pattern and peak positions reported by other researchers in literature.

The average crystallite particle size was examined to be 41.5 nm from the XRD patterns of the developed catalyst using Scherer equation 2 (Chen *et al.,* 2006) and the percentage abundance is shown in Figure 3.

$$D = \frac{K\lambda}{\beta COS\theta} \qquad 2$$

Where D is the particle size diameter,β is the full width at half maximum, λ is the wave length of X-ray, θ is the diffraction angle and K is the Scherer constant.

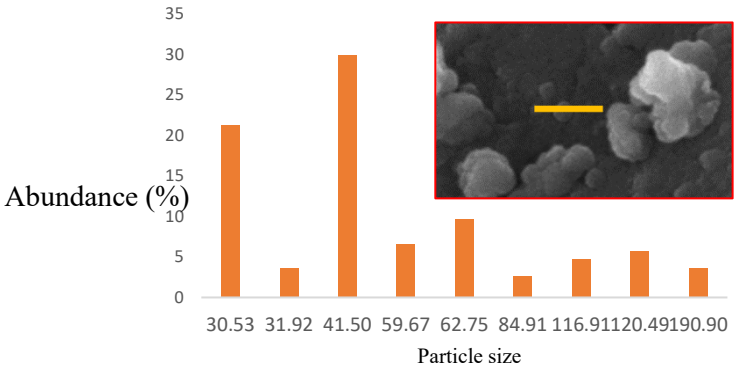

Figure 3: Percentage Crystallite Size Population Density of Catalyst

From Figure 3 it can be seen that majority of the particle fall within 41.50 nm which confirmed that the size of the prepared monometallic catalyst is nanostructure in nature and as such the catalyst is a good template for CNTs production. The result of the average crystalline particle obtained (82.18 nm) shows a quite deviation from that obtained by kariim *et al.* (2015) with obtained average particle size of 42.24 nm from their XRD analysis.

The HRSEM image presented in Figure 4 indicates that the clustered solid catalyst material is near spherical in geometry and is of high crystallinity. The agglomerates seen in the SEM images could be ascribed to the drying process in sample preparation. The micropores can be recognized in the catalyst, a property showing that there was appropriate dispersion of Ni nanoparticles on the Al_2O_3 support material with tiny spaces inside the composite. The Al_2O_3 matrix sites were homogeneously occupied by the oxides of Ni that was formed during calcination of the catalyst sample. The SEM image of the catalyst also indicates that the nickel nanoparticles that were dispersed on the Al_2O_3 support material are suitably less than 50 nm in size (red arrow, concentric square). The results also show that nitrates of nickel nitrate salts were effectively removed by converting them to oxides during calcination. Though, there are little clusters of nanoparticles (red arrow, lower right-hand corner) and lumps of catalyst (yellow arrow). These might be responsible for the growth of CNTs of varying diameter, which is one of the existing challenges in producing nanotubes of uniformly distributed diameter from catalyst prepared by wet impregnation.

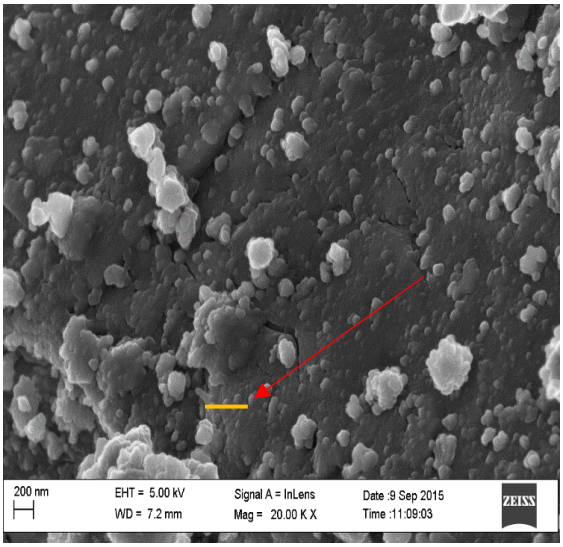

Figure 4: SEM image showing nanoparticles of Ni dispersed on Al_2O_3 support

The surface area analysis was carried out on the developed monometallic nickel catalyst (Ni/Al_2O_3) by BET method. The SBET surface area of the developed monometallic catalyst was determined to be 428.352 m^2/g using the multipoint equation under nitrogen condition, with micropore volume of 0.1779 cc/g and micropore half pore width of 28.17 Â. This surface area is little less than those reported by (Abassi *et al.,* 2014). This may be due to the presence of weak bond that exist between $Ni\text{-}Al_2O_3$ (Zhang *et al.,* 2006).

The HRTEM micrograph of the produced CNTs is presented in Figure 5. The micrograph shows a densely populated strand of CNTs with high degree of homogeneity covering the impurity present. The morphology of the CNTs illustrates that the CNTs formed under these conditions are entangled with each other and possess curved, hollow, and tubular shapes, with diameters in the range of 15 – 45 nm. Also, some catalyst particles appear to be encapsulated within the nanotubes hollow core. Encapsulated metal nanoparticles are also detected along the inside diameter of the nanotubes samples which were introduced by the metal catalysts utilized for CNTs growth.

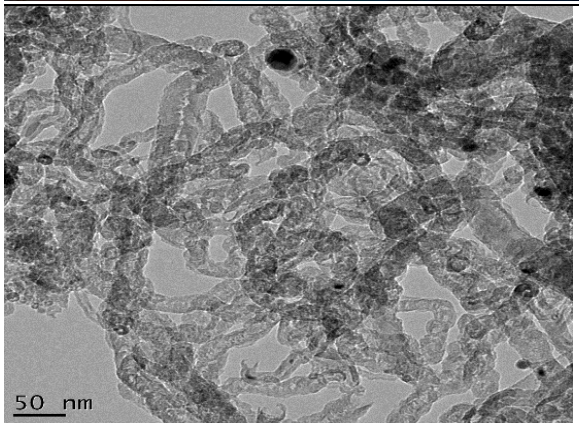

Figure 5: TEM image of as-synthesized MWCNTs

Figures 6 represents the TGA and DTA profile of as-produced MWCNTs which were attained under N_2 environment and heating rate of 10 ^{0}C /min up to 900 ^{O}C. It can be deduced from the result that the loss of absorbed moisture on the as-synthesized CNTs was responsible for the weight loss between 30 -100 ^{o}C, while the reduction observed at the temperature of 100 - 400 ^{o}C depicts the removal of crystal water of nitrates and elimination of volatile products. Between 400 -800 ^{o}C, the change of weight was not significant beyond which the CNTs exhibited another regime of steady weight loss. The percentage weight loss of the as-synthesized CNTs observed are 10 % (30 -100 ^{o}C), 20 % (100 – 400 ^{o}C), 21 % (400 – 800 ^{o}C) and 40 % (800 – 950 ^{o}C).

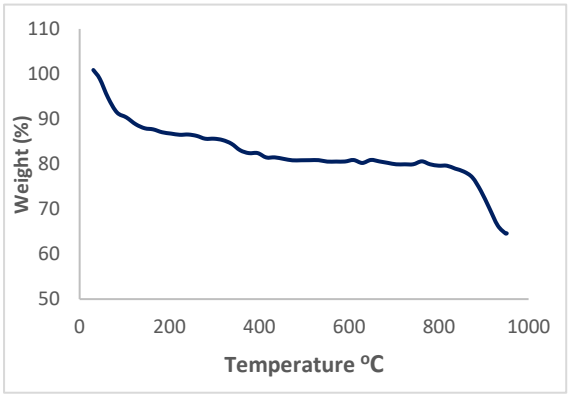

Figure 6: TGA Profile of As-synthesiseed CNTsobtained at 10 ^{O}C/min heating rate under Nitrogen atmosphere.

The loss in weight of the as-synthesized MWCNTs is associated to the presence of impurities that oxidizes at temperatures lower than that of nanotubes which accompany the synthesis of the CNTs (Ebbensen *et al.,* 1994; Eftehari *et al.,* 2005) and these impurities are in the form of amorphous carbon and metals.

Utilizing the hydrodynamic diameter of the sample as obtained by DLS, the literature values of aspect ratio of MWCNT was used to correlate length and diameter of this single CNT sample. Z-average (or hydrodynamic diameter) of the sample represents neither the diameter nor the length of the nanotube. The correlated equation utilized for the determination of length and diameter based on these aspect ratios is (Nair *et al.*, 2008; Horiba Ltd, 2015).

$$Dh = \frac{L}{In(\mathrm{L/d}) + 0.32}$$

Aspect ratio of MWCNTs produced by CVD process as reported by Abu Al-Rub, Ashour & Tyson (2012), ranges from 157 to 3,750. These values of aspect ratio (L/d), along with Z-average from DLS were substituted to find the corresponding lengths and diameters of the as-grown MWCNT produced in the current work. This analyses provides a correlation between the diameter, length and aspect ratio, for this MWCNT sample, as shown in the charts of Figures 7.

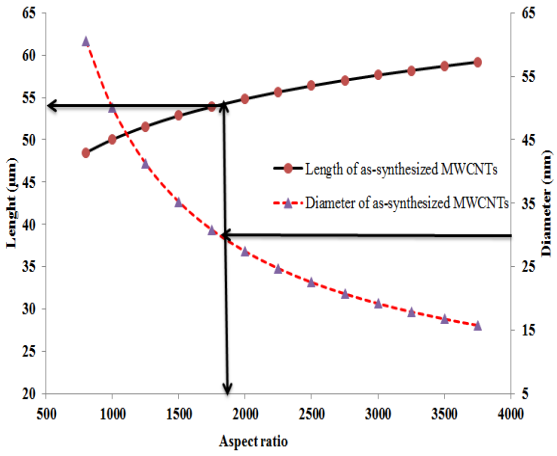

Figure 7: Correlation chart between the aspect ratio, length and diameter of the as – grown MWCNT sample.

Specific surface area m_2/g of the synthesized is presented in Table 1 the SBET surface area of the as synthesized CNTs was determined to be 833.64 m^2/g

using the multipoint equation under nitrogen condition, with micro pore volume of 0.3286 m^3/g and micro pore half pore width of 31.48 Â. This surface area is a little high than those reported by (Abassi *et al.,* 2014). This may be due to the presence of weak bond that exist between Ni-Al_2O_3 (Zhang *et al.,* 2006). Peigney *et al.* (2001) also showed that the surface area of MWNTs decreases with increasing walls and nanotube diameters. However, the trend of the surface area obtained in this work do not strictly obey the observation made by Peigney and co-workers because the average sizes are affected by contribution from sizes of impurities present in varying quantities in the samples.

Table 1: Result showing BET-Surface area Analysis

Surface area, pore volume, pore size of synthesized CNTs and average particle size

BET surface area (m^2/g)	833.641
Pore volume (m^3/g)	0.3286
Pore size (Â)	0.3148
Average Particle size (DLS) nm	82.24

The SAED patterns of the CNTs sample confirmed the graphitic nature of MWCNTs especially the innermost ring which is due to the usual strongest reflection plane (002) of graphite (Das e*t al.*, 2015). As illustrated in Figure 8. The occurrence of the sharp rings at reciprocal lattice spacing (1/*d*) of 2.9, 4.8, 5.7 and 8.5 nm^{-1} are in good agreement with those reported for graphite. Kariim, (2015) also collected SAED pattern of MWCNTs and observed sharp rings attributable to the MWCNT at reciprocal lattice spacing of 3.1, 5.0, 6.0 and 8.5 nm^{-1}.

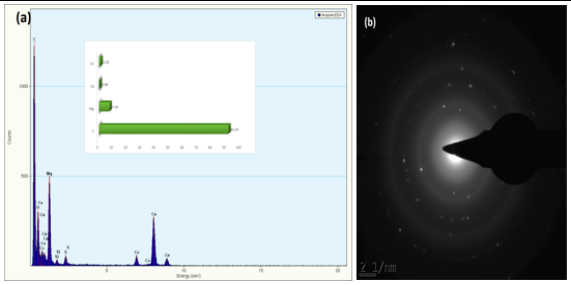

Figure 8: (a) EDS and (b) SAED pattern of as-synthesized MWCNTs

Again, it can be observed from the SAED that the CVD reaction parameters affect the crystallinity of MWCNTs and it present a low crystallinity which as it displayed diffuse rings in its SAED pattern, which is typical of amorphous substances. The single bright spots are reflections from certain individual crystals.

4.0 CONCLUSION

In this study, multi-walled carbon nanotubes were successfully produced from nickel supported alumina catalyst via wet impregnation followed by CVD technique. The CNTs was successfully synthesized at reaction time of 45 minutes, temperature of 600 ºC, argon flow rate of 200 ml/min and acetylene flow rate 100 ml/min. The average diameter of the as-produced multiwalled carbon nanotubes obtained from bimetallic Ni/Al_2O_3 catalyst was 28.89 nm whereas; the bimetallic catalyst had average particle size of 46.24 nm. The correlation chart showed that the MWCNTs produced was a long-tube multiwall carbon nanotubes with aspect ratio of 1250. Thus, the nickel catalyst on alumina support developed via incipient wet impregnation method is suitable for CNTs production by CVD method.

REFERENCE

Abbasi, N., and Mahdavifar, Z. (2014). The influence of
Cu-doping on aluminum nitride, silicon carbide and boron nitride nanotubes' ability to detect carbon dioxide; DFT study. *Physica E: Low-dimensional Systems and Nanostructures*, *56*, 268-276.
Abbasi, S. A., Loan, S. A., Nizamuddin, M., Bashir, F., Shabir, H., Murshid, A. M., R., and Alamoud, A. (2014). Design of a novel high gain carbon

nanotube based operational transconductance amplifier. In *Proc. of the International MultiConference of Engineers and Computer Scientists 2014-IMECS 2014*.

Afolabi, A. S., Abdulkareem, A. S., Mhlanga, S. D. and Iyuke, S. E. (2011) "Synthesis and purification of bimetallic catalysed carbon nanotubes in a horizontal CVD reactor", *Journal of Experimental Nanoscience, vol. 6(3), 248-262*

Ajayan, P.M. and Zhou, O.Z. (2001), Applications of carbon nanotubes. *Carbon Nanotubes (Topics in Applied Physics), ed Dresselhaus, M.S., Avouris, Ph. 80, 391-425*, Berlin: Springer Verlag.

Arranz-Andréas, J., and Blau, W. J. (2010). Enhanced device performance using different carbon nanotube types in polymer photovoltaic devices. *Carbon*, *46*(15), 2067-2075.

Awadallah, A. A., Mina, A. N., Phillips, A. H., and Ahmed, R. R. (2012, February). Simulation of the Band Structure of Graphene and Carbon Nanotube. In *Journal of Physics: Conference Series* (Vol. 343, No. 1, p. 012076). IOP Publishing.

Baughman, R. H., Zakhidov, A. A., Heer, W. A. (2002) Carbon nanotubes-the route toward applications. Science, 297 pp.787-792.

Bondi, S. N., Lackey, W. J., Johnson, R. W., Wang, X. and Wang, Z. L. (2005), Laser assisted chemical vapour deposition synthesis of carbon nanotubes and their characterization, *Carbon* 44 (2006) 1393–1403. doi:10.1016/j.carbon.2005.11.023

Chen, G. Z., Shaffer, M. S., Coleby, D., Dixon, G., Zhou, W., Fray, D. J., and Windle, A. H. (2006). Carbon nanotube and polypyrrole composites: coating and doping. *Advanced Materials*, *12*(7), 522-526.

Ebbesen, T. W., Treacy, M. J., and Gibson, J. M. (1996). Exceptionally high Young's modulus observed for individual carbon nanotubes.

Esfarjani S.A (2013). A Modeling Framework for the Synthesis of Carbon Nanotubes by Plasma Technology. Published PhD Thesis. University of Toronto, Canada.

Horiba Scientific Ltd (2015), "Carbon nanotube particle size". Available online at http//www.horiba.com/scientific/products/particle-characterization/applications/carbon-nanotubes/. Retrieved May, 2015.

Kariim I, Abdulkareem, A.S., Abubakre O.K., Mohammed, T.A., Bankole, M.T and Jimoh T. (2015). Suitability of Alumina (Al_2O_3) as Bimetallic Catalyst Support for MWCNT Growth. *Journal of Nanotechnology*, 1 - 16.

Kathyayini, H., Reddy, K. V., Nagy, J. B., and Nagaraju, N. (2008). Synthesis of carbon nanotubes over transition metal ions supported on Al (OH) 3. *Indian journal of chemistry. Section A, Inorganic, bio-inorganic, physical, theoretical & analytical chemistry*, *47*(5), 663.

Muhammad M. A., Javed I., (2011). Production of Carbon Nanotubes by Different Routes— A Review. *Journal of Encapsulation and Adsorption Sciences, 2011, 1, 29-34*, 29-34

Nair, N., Kim, W., Braatz, R., and Strano, M. (2008) *Langmuir*, 24, 1790 – 1795

Peigney, A., Laurent, C., Flahaut, E., Bacsa, R. R., & Rousset, A. (2001). Specific surface area of carbon nanotubes and bundles of carbon nanotubes. *Carbon*, *39*(4), 507-514.

Qian, D., Liu, W. K., & Ruoff, R. S. (2009). Load transfer mechanism in carbon nanotube ropes. *Composites Science and Technology*, *63*(11), 1561-1569.quantumdotled. html. Accessed July 10, 2006

Toussi, S. M., Fakhru'l-Razi, A., Chuah, A., and Suraya, A. (2011). Effect of synthesis condition on the growth of SWCNTs via catalytic chemical vapour deposition. *Sains Malaysiana*, *40*(3), 197-201.

Uddin, M. A., Tsuda, H., and Sasaoka, E. (2008). "Catalytic Decomposition of Biomass Tars with Iron oxides Catalyst", Fuel, Vol. 87, No (4), pp. 451-459.

Yeoh, Wei-Ming; Lee, Kim-Yang; Chai, Siang-Piao; Lee, Keat-Teong; & Mohamed, A. (2009). Synthesis of high purity multi-walled carbon nanotubes over Co-Mo/MgO catalyst by the

Zhang, Q., Yu, H., Zhang, Q., Wang, Q., Ning, G., Luo, G. and Wei, F. (2006), "Effect of the reaction atmosphere on the diameter of single-walled carbon nanotubes produced by chemical vapour deposition". *Carbon, 44, pp. 1706–1712.*